Int. J. Electrochem. Sci., 8 **(2013)** 6502 - 6512

International Journal of
ELECTROCHEMICAL
SCIENCE
www.electrochemsci.org

An Amperometric Hydrogen Peroxide Biosensor Based on Myoglobin Immobilized on SDS-GNPs-GR Modified Electrode

Miao-Qing Xu, Jian-Feng Wu, Guang-Chao Zhao[*]

School of Environmental Science, Anhui Normal University, Wuhu, 241000, P R China
[*]E-mail: gczhao@mail.ahnu.edu.cn

Received: 28 March 2013 / *Accepted:* 15 April 2013 / *Published:* 1 May 2013

Chemically reduced graphene and gold nanoparticles composites were obtained using sodium dodecyl sulfate (SDS) as stabilizing agent and successfully dispersed fully in water to form a stable black aqueous solution. The as-prepared graphene and gold nanoparticles composites were successfully immobilized on electrode surface to construct a SDS-GNPs-GR modified electrode. The composites showed an obvious promotion of the direct electron transfer between myoglobin (Mb) and the underlying electrode. The experimental results also clarified that the adsorbed Mb retained its biological activity toward the reduction of hydrogen peroxide with high sensitivity and fast response. The biosensor possesses a linear response range of 0.45-8.1μM H_2O_2 with a correlation coefficient of 0.9989 and a detection limit of 1.2×10^{-8} M based on a signal-to-noise ratio of 3.

Keywords: Myoglobin, Graphene, Gold nanoparticles, Biosensor.

1. INTRODUCTION

Electrochemical biosensors are generally defined as analytical devices which convert a biological response into a quantifiable and processable electrical signal. They are of particular interest because of practical advantages, such as operation simplicity, low expense of fabrication, and suitability for real-time detection. Up to now, studies on the direct electron transfer (DET) between redox proteins and electrode surface have attracted considerable attention, because it can not only provide a model for the mechanistic study of biological electron transport but also enable the establishment of non-mediator biosensors and enzymatic bioreactors [1, 2]. Myoglobin, a kind of heme proteins, is a single-chain globular protein that consists of 153 amino acids and a heme group (an iron-containing porphyrin). It is an ideal model molecule for the study of electron transfer reactions of heme proteins and biosensing [3, 4]. However, it's difficult for Mb to exhibit heterogeneous electron-

transfer process in most cases, which means that the rate of electron transfer of Mb is very slow. Great efforts have been made to facilitate the direct electron transfer of heme proteins by modifying the electrodes using mediators, promoters, or other functional materials [5-13].

Graphene is a one-atom-thick planar sheet of sp^2-bonded carbon atoms densely packed in a honeycomb crystal lattice. The unique feature of graphene, the ‘‘thinnest’’ known material, has attracted tremendous interest both in academics and industry. Recently, graphene has been used as alternative carbon-based nanofiller in the preparation of polymer nanocomposites [14-21]. Among these, many efforts have been devoted to improve the capability of chemically reduced graphene (cr-GR) through association of cr-GR with metallic nanoparticles since metallic nanoparticle-carbon composites have attracted tons of interest in electrochemical sensors and catalysts [22-25].

As well known, gold nanoparticles (GNPs) is one of the most intensively studied and applied metal nanoparticles in electrochemistry due to their extraordinarily physical and chemical properties [26-28]. These unique properties allow them to facilitate charge transfer between electrode and enzyme and construct electrochemical sensors [29, 30]. Herein, Graphene-GNPs nanocomposite has been used to preparation electrochemical biosensor. For example, Niu et al [31] have constructed a novel glucose biosensor based on immobilization of glucose oxidase in nanocomposites of graphene and gold nanoparticles at a gold electrode. Huang et al [32] also studied that the GNPs/graphene-NH_2 nanocomposite could effectively facilitate the direct electron transfer of catalase to the electrode. To the best of our knowledge, there have been few reports about the application of graphene-GNPs composite for immobilization of redox proteins.

In this work, we synthesized gold nanoparticles using graphene oxide (GO) as protecting agent to obtain gold nanoparticles-graphene oxide composites. The subsequent chemical reduction of graphene oxide composites employed sodium dodecyl sulfate (SDS) as an effective disperser to isolating graphene (GR) nanosheets modified with gold nanoparticles from each other. SDS, a kind of surfactant, has a similar amphoteric structure as lipid, which makes it possible to form a stable membrane the same as a lipid membrane and can be used to embed proteins. The as-prepared SDS-dispersed graphene nanosheets modified with gold nanoparticles were cast on the surface of electrode to form a SDS-GNPs-GR modified electrode, which was used to immobilize myoglobin (Mb). The electrochemical and electrocatalytic properties of the immobilized Mb were characterized.

2. EXPERIMENTAL

2.1. Apparatus and reagents

Electrochemical experiments were performed with CHI660 electrochemical analyzer (CHI, USA) with a conventional three-electrode cell. The Mb/SDS-GNPs-GR modified basal plane graphite (BPG) electrode (Φ = 5.2 mm) was used as a working electrode. An Ag/AgCl electrode and a platinum wire electrode were used as the reference and the auxiliary electrodes, respectively.

Horse heart Myoglobin was obtained from Sigma and used without purification. Mb solution (5 mg mL^{-1}) was stored at 4^oC as stock solutions. Graphite, hydrazine hydrate solution (50 wt %) was

purchased from Shanghai Chemical Reagent Co. Ltd. H_2O_2 is the product of Beijing Chemical Reagent Factory (Beijing, China). Other chemicals were of analytical grade and used without further purification. All solutions were made up with doubly distilled water and purged with high-purity nitrogen for at least 10 min prior to each electrochemical experiment, and a nitrogen atmosphere was maintained over the solution during the measurement process. Scanning electron microscopy (SEM) image was obtained using a LEO1530 field emission SEM system (Germany).

2.2. Synthesis of gold nanoparticles in graphene oxide suspension

The oxidation of the graphite was carried out based on the Hummers method [33]. The obtained graphene oxide was washed with deionized water six times to remove the remaining metal ions and acid and stored for use. We prepared GNPs-GO nanocomposites by chemical reduction of $HAuCl_4$ with $NaBH_4$ in the presence of graphene oxide. An aqueous solution of $HAuCl_4$ (40 μL, 58 mM) was added into graphene oxide aqueous solution (4 mL, 0.45 mg mL^{-1}) and stirred for 5 minutes. After that, slow and controlled addition of $NaBH_4$ aqueous solution (40 μL, 0.2 M) is essential to avoid gold nanoparticles forming too fast to aggregate.

2.3 Chemically reduction of GNPs-GO nanosheets

SDS solution (1mL, 0.1M) was mixed into the GNPs-GO suspension and stirred for 20 minutes. Subsequently, 20μL hydrazine hydrate solution was added to that solution and stirred for 5 min. At last, this mixture was reacted at 100°C for 24 hours. After the hydrazine-vapor treatment, the GNPs-GO solution changed color, from red to black, indicating the reduction of the graphene oxide. The resulting black solution (denoted as SDS-GNPs-GR) can remained their fine dispersion at least three months.

2.4 Electrode preparation

Initially, the BPG electrode was carefully polished with abrasive paper before each experiment. After a short rinse with distilled water and ultrasonic cleaning with distilled water and ethanol, the electrode was allowed to dry at room temperature. Then, 10μL SDS-GNPs-GR suspension was cast on the surface of the pretreated BPG electrode with a microsyringe and the solvent (water) was allowed to evaporate at ambient temperatures. The obtained electrode was denoted as SDS-GNPs-GR/BPG electrode. Finally, SDS-GNPs-GR/BPG electrode was incubated in phosphate buffer solution (pH 7.0) containing 5 mg mL^{-1} Mb for 3h to form an Mb/SDS-GNP-GR/BPG electrode. Prior to electrochemical experiments, the modified electrode was rinsed thoroughly with doubly distilled water and stored at 4^oC.

3. RESULTS AND DISCUSSION

3.1 Characterization of the GNPs-GO composites

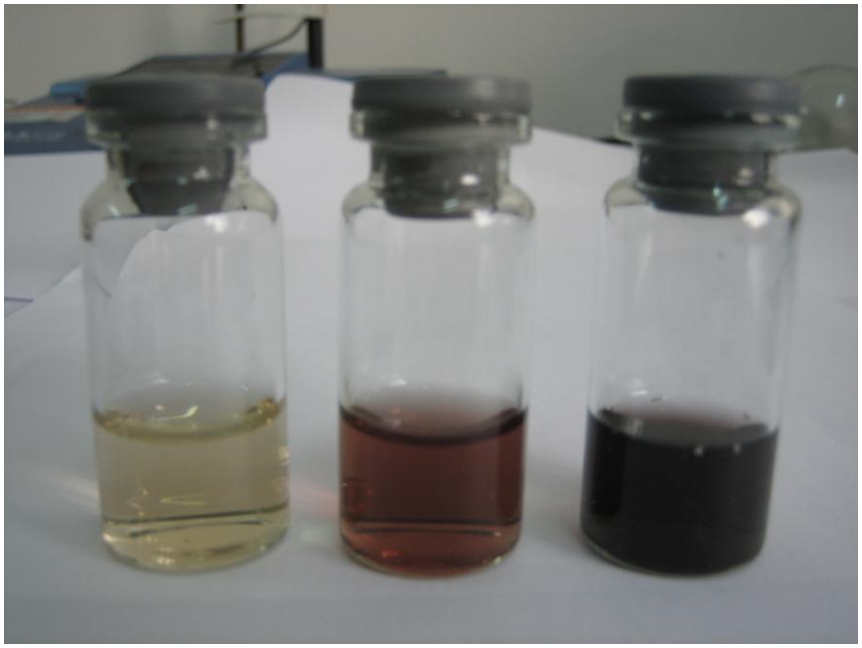

Figure 1. Photograph of graphene-oxide, gold nanoparticles-graphene oxide and gold nanoparticles-graphene composites solutions (from left to right).

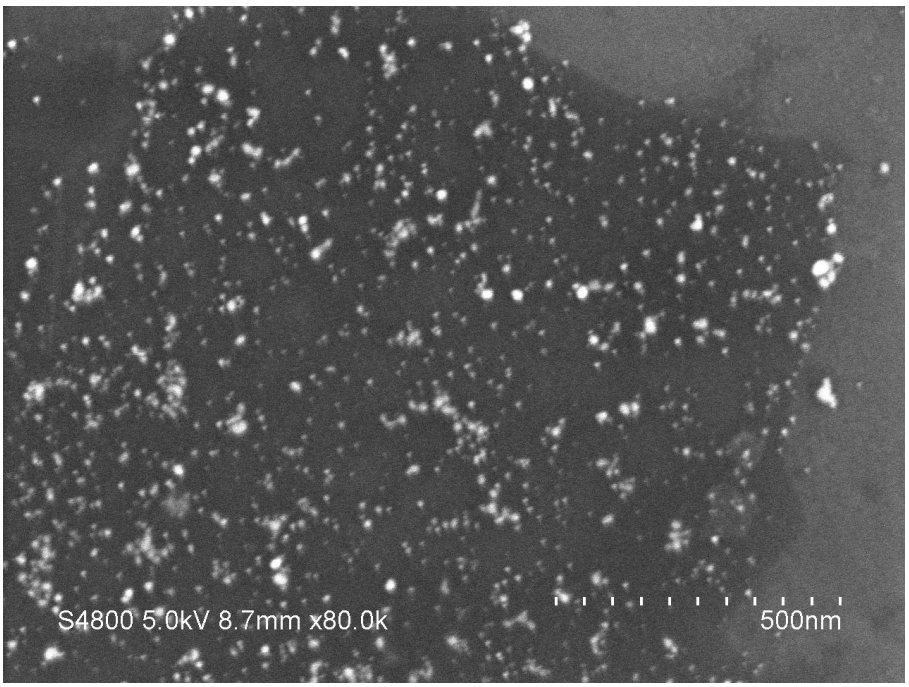

Figure 2. SEM image of gold nanoparticles-graphene nanocomposites.

Photographs of graphene-oxide, gold nanoparticles-graphene oxide composite and gold nanoparticles-graphene composite solutions are shown in Fig. 1, left to right respectively. The obtained

aqueous solution of graphene oxide based on the Hummers method brought out light yellow. The gold nanoparticles-graphene oxide composite solution created a red wine color, indicating that individual small gold nanoparticles were formed. In also testifies that the graphene-oxide plays an important role in regulating the size of gold nanoparticles. Subsequently, we added hydrazine hydrate to GNPs-GO solution to obtain a GNPs-GR solution in the presence of sodium dodecyl sulfate. The gold nanoparticle-graphene solution turned to black, which is clear evidence of the reduction of graphene oxide.

Fig. 2 depicts scanning electron micrograph (SEM) of the GNPs-GR composites. It can be seen that gold nanoparticles are uniformly distributed on the surface of graphene nanosheet with a size of less than 40 nm. This fact showed that the presence of the oxygen functionalities at the graphene surface plays an important role on the nucleation and growth of gold nanoparticles.

3.2. Direct electrochemistry of Mb on SDS-GNPs-GR/BPG electrode

The electrochemical behaviors of SDS-GNPs-GR/BPGE and Mb/SDS-GNPs-GR/BPGE in Mb-free phosphate buffer solution (0.1 M, pH 7.0) were studied by cyclic voltammetry.

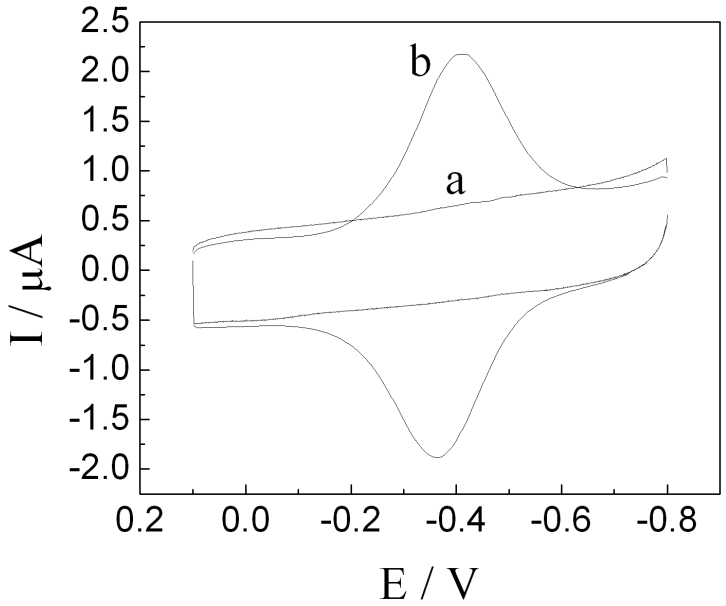

Figure 3. Typical CVs of (a) SDS-GNPs-GR/BPG electrode and (b) Mb/SDS-GNPs-GR/BPG electrode in 0.1 M PBS, pH 7.0, with a scan rate of 100 mV s^{-1}.

As shown in Fig.3, no redox peaks were observed using SDS-GNPs-GR/BPG electrode as the working electrode (Fig. 3a). The Mb/SDS-GNPs-GR/BPG electrode showed a couple of stable and well-defined redox peaks and the separation of anodic and cathodic peak potentials is 53 mV (curve b in Fig. 3). The shapes of the redox peaks were symmetric and the peak currents of anode and cathode were essentially equal, suggesting that electroactive Mb on the electrode surface are reduced on the forward negative scan and are oxidized fully again when the potential scan was reversed. The

experimental results indicated that the combination of graphene and gold nanoparticles have a significant effect on the kinetics of the electrode reaction for the proteins and provide a suitable network-like microenvironment for the proteins to transfer electrons to the BPG electrode.

Fig.4 illustrates the cyclic voltammograms (CVs) of Mb/SDS-GNPs-GR modified electrode at different scan rates range from 0.06 to 0.3 V s^{-1}. As can be seen, both cathodic and anodic peak currents increased linearly with the scan rate with a correlation coefficient of 0.9959, suggesting that this is a surface-controlled process. The electron transfer rate constant (*Ks*) can be estimated according to Laviron [34], which is 24.4s^{-1}**.** The *Ks* value indicates that SDS-GNPs-GR composite is an excellent promoter for the electron transfer between Mb and electrode. According to the slope of the Ip-v curve and the equation of $I_p = n^2F^2vA\Gamma^*/4RT$ [35], the average surface concentration (Γ^*) of electroactive Mb entrapped on the SDS-GNPs-GR modified electrode was calculated to be $(6.51\pm0.3)\times10^{-11}$ mol cm^{-2}, suggesting an approximate monolayer of Mb adsorbed on the surface of SDS-GNPs-GR electrode.

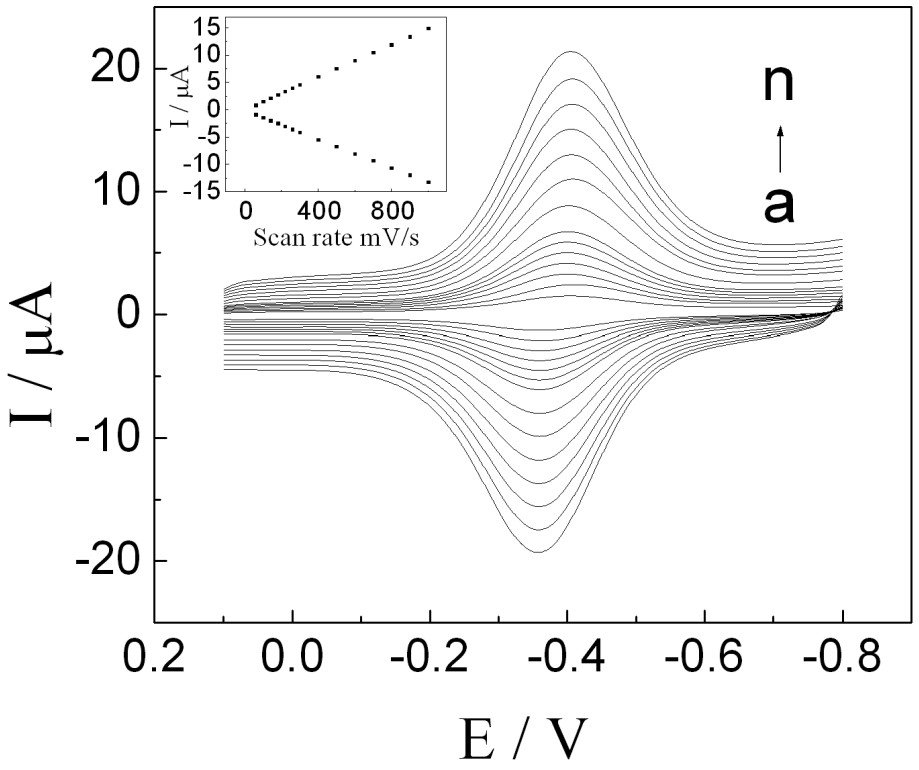

Figure 4. CVs of the Mb/SDS-GNPs-GR/BPG electrode in N_2-saturated PBS (pH 7.0) at different scan rates. Scan rate (from a to n): 0.06, 0.1, 0.14, 0.18, 0.22, 0.24, 0.3, 0.4, 0.5, 0.6, 0.7, 0.8, 0.9 and 1.0 V s^{-1}. Inset: The dependence of anodic and cathodic peak currents vs. scan rate in the range 0.06-1.0 V s^{-1}.

The effect of the pH of the supporting electrolyte on the peak potentials of the Mb was also investigated. Both reduction and oxidation peak potentials of the heme Fe (III)/Fe (II) redox couples for the Mb-SDS-GNPs-GR film are obviously dependent on the pH value in the range of 5.0 to 9.0. The apparent formal potential of the Mb heme Fe (III)/Fe (II) redox couple, which were estimated as

the midpoint of cathodic and anodic peak potentials, had shifted linearly to the negative direction with the increase of pH value with a slope of -51.6 mV pH^{-1}. This value is reasonably close to the theoretical value of-59 mV pH^{-1} unit expected for a reversible one electron transfer coupled by single proton transportation [36]:

Mb heme Fee(III) + H^+ + e^- →Mb heme Fe(II)

Subsequently, the same CVs obtained at pH 7.0 could reproduce when the same modified electrode back to the pH 7.0 buffer. This was likely due to a reversible pH-induced conformational change of Mb at low pH.

3.3. Electrocatalytic activity of Mb/SDS-GNPs-GR/BPG electrode for the reduction of hydrogen peroxide

Based on the direct electrochemistry of the protein, the composites can offer great advantages to fabricate a biosensor. Fig. 5 depicts CVs of the Mb/SDS-GNPs-GR/BPG electrode in the absence and the presence of H_2O_2. At a bare BPGE, no peaks can be observed (Fig. 5a). However, at Mb/SDS-GNPs-GR/BPG electrode, an obvious catalytic reduction peak appeared at -0.318V. The cathodic peak current of Mb increased and its anodic peak current decreased with increasing the concentration of H_2O_2 (as shown in b-f in Fig. 5), showing a typical electrocatalytic reduction process. The catalytic activity of Mb shows that Mb is partly unfolded.

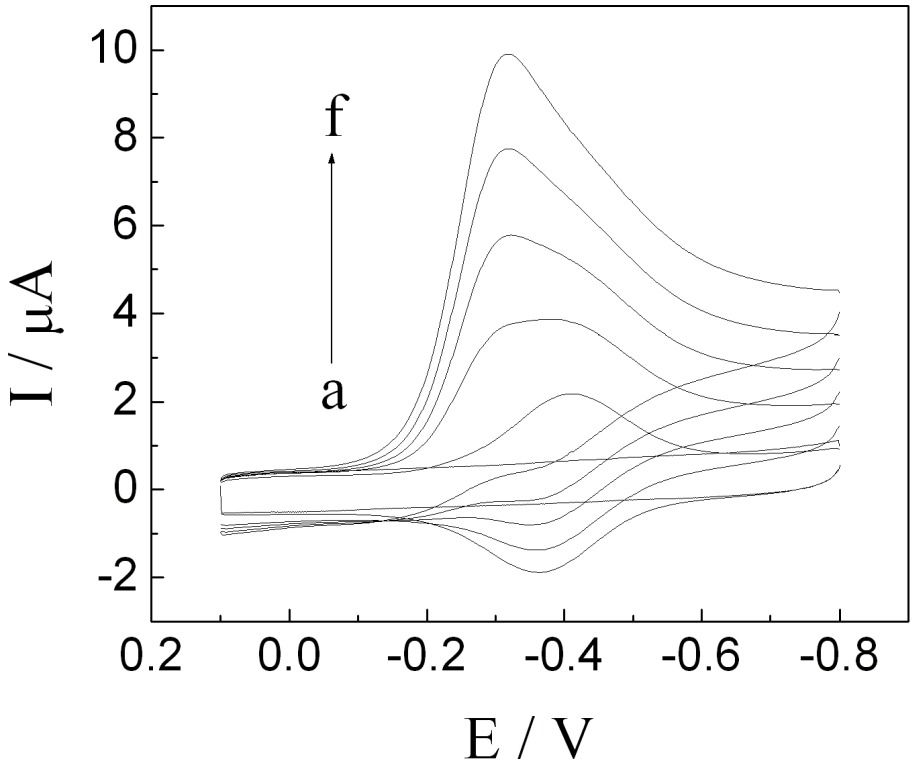

Figure 5. CVs of BPGE (a: 0.02 mM H_2O_2) and Mb/SDS-GNPs-GR/BPGE in PBS (pH 7.0) containing H_2O_2 (b) 0, (c) 0.02, (d) 0.04, (e) 0.06 and (f) 0.08 mM. The scan rate is 100 mV s^{-1}.

The amperometric response of the Mb/SDS-GNPs-GR/BPG electrode toward H_2O_2 was recorded through successively adding H_2O_2 to a continuous stirring PBS solution. In this process, a potential of -0.30V was applied to the working electrode. As displayed in Fig. 6, the reductive current increases to reach a stale plateau within 3 s when adding H_2O_2 into the buffer solution. This indicated that the response of the electrode to H_2O_2 should be a quick responsive process. The calibration plot for the H_2O_2 determination was constructed. Its linear segment increases from 0.45μM to 8.1μM, with a correlation coefficient of 0.9989. The detection limit for the determination of H_2O_2 was obtained as 1.2×10^{-8} M at S/N=3. The result suggests that the Mb/SDS-GNPs-GR/BPG electrode can be used as a reagentless biosensor to detect H_2O_2. In addition, determined parameters of this sensor compared with other modified electrodes used for the determination of H_2O_2 are represented in Table 1. Compared with the existing reports about determination of H_2O_2 [37-42], this method is convenient to prepare the Mb/SDS-GNPs-GR/BPG modified electrode and has high sensitivity, wide linear range and good repeatability.

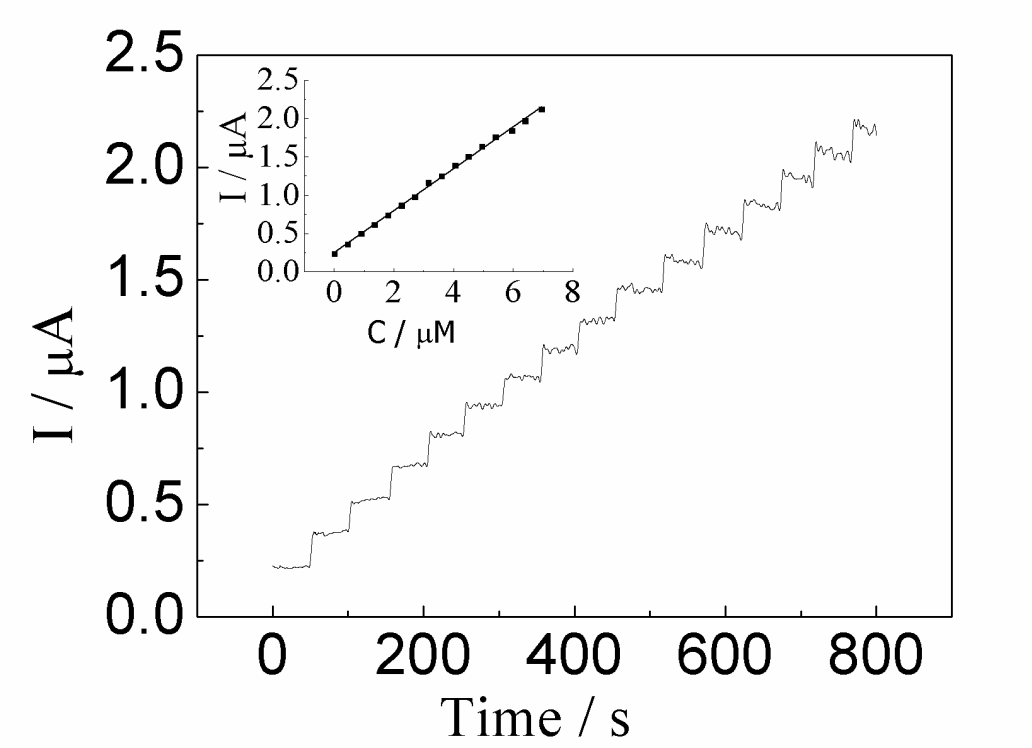

Figure 6. Amperometric response of Mb/SDS-GNPs-GR/BPG electrode towards H_2O_2. Conditions: a -0.30 V constant potential modulated with 50 mV pulse in the time intervals of 0.5 s; successive additions of 10 μL of 0.5 mM H_2O_2 to 10 mL of 0.1 M PBS, pH 7.0, and the stirring rate is 400 rpm. Inset: the dependence of peak currents on the concentrations of H_2O_2.

3.4. Stability and reproducibility of the biosensor

The stability of the electrode was investigated. Even though 400 continuous cyclic scans were carried out in the potential range from 0.1 V to -1.0 V at a scan rate of 100 mV s^{-1}, no obvious change of CV curve can be observed, suggesting that proteins can tightly immobilized on the surface of

modified electrode. Eight repetitive experiments were carried out with the buffer solution containing 8 μM H_2O_2. The relative standard derivation for eight repetitive measurements was found to be 2.1%. When the Mb/SDS-GNPs-GR modified electrode was stored in a pH 7.0 PBS for at least 4 weeks at 4 °C, the electrode retained more than 86% of its reduction current towards H_2O_2.

Table 1. Comparison of the proposed method with other electrochemical methods for determination of H_2O_2

Electrode	Linear range (M)	Detection limit (M)	Ks (s^{-1})	Reference
Nafion/Myoglobin/ionic liquid/ modified glassy carbon electrode	1.0×10^{-6}~ 1.8×10^{-4}	1.4×10^{-7}	—	[37]
Nafion/ tetrasodium 1,3,6,8-pyrenetetrasulfonic acid – horseradish peroxidase modified glassy carbon electrode	6.3×10^{-7}~ 1.68×10^{-5}	1.05×10^{-7}	3.5	[38]
horseradish peroxidase / multi-walled carbon nanotubes/electro-copolymerized nano-Pt-poly(neutral red) modified glassy carbon electrode	3.6×10^{-6} ~4.3×10^{-3}	1.1×10^{-6}	1.83	[39]
hemoglobin (Hb)–collagen microbelt modified electrode	5.0×10^{-6}~ 3.0×10^{-5}	3.7×10^{-7}	270.6	[40]
hemoglobin–monoolein modified glassy carbon electrode	7.0×10^{-7}~ 2.39×10^{-5}	3.1×10^{-6}	3.03±0.03	[41]
Hb /didodecyldimethylammonium bromide modified powder microelectrode	1.0×10^{-6}~1.43×10^{-5}	2.3×10^{-7}	2.99	[42]
myoglobin / sodium dodecyl sulfate / gold nanoparticles/ graphene modified basal plane graphite electrode	5.0×10^{-7}~7.5×10^{-6}	1.2×10^{-8}	24.4	This work

4. CONCLUSION

In conclusion, Mb adsorbed on the SDS-GNPs-GR modified electrode via the electrostatic interactions retains its native secondary protein structure and the direct electron transfer was achieved. The CVs of Mb/SDS-GNPs-GR modified electrode exhibited a pair of redox peaks corresponding to the electroactive center of Mb with a single proton transfer. Moreover, the immobilized Mb displayed excellent electrocatalytic activity for the reduction of H_2O_2. Based on these, a new biosensor was constructed and SDS-GNPs-GR composites could also be exploited for the improvement of analytical performance of other biosensors.

ACKNOWLEDGEMENTS
The authors thank the National Natural Science Foundation of China (20975001) for fund support.

References

1. S.R. Santos, G. Maia, *Electrochim. Acta* 71 (2012) 116.
2. H.N. Guan, Fuli Zhangc, J. Yu, D.F. Chi, *Food Res. Int.* 49 (2012) 15
3. M.Z. Wang, Q.L. Sheng, D.W. Zhang, Y.P. He, J.B. Zheng, *Bioelectrochemistry* 86 (2012) 46
4. S.Y. Dong, N. Li, T.L. Huang, H.S. Tang, J.B. Zheng, *Colloids and Surfaces B* 173 (2012) 704
5. C.X. Ruan, T.T. Li, Q.J. Niu, M. Lu, J. Lou, W.M. Gao, W. Sun, *Electrochim. Acta* 64 (2012) 183
6. C.C. Guo, H. Sun, X.S. Zhao, *Sensor. Actuat. B-Chem.* 164 (2012) 82
7. S. Lata, B. Batra, N. Karwasra, C. S. Pundir, *Process Biochem.* 47 (2012) 992
8. W. Wang, T.J. Zhang, D.W. Zhang, H.Y. Li, Y.R. Ma, L.M. Qi, Y.L. Zhou, X.X. Zhang, *Talanta* 84 (2011) 71
9. Y. Ke, Y. Zeng, X.L. Pu, X. Wu, L.F. Li, Z.H. Zhu, Y. Yu, *RSC Advances* 2 (2012) 5676
10. X.M. Sun, Y. Zhang, H.B. Shen, N.Q. Jia, *Electrochim. Acta* 56 (2010) 700
11. T.R. Zhan, Y.Q. Guo, L. Xu, W.L. Zhang, W. Sun W.G. Hou, *Talanta* 94 (2012) 189
12. H.P. Peng, R.P. Liang, L. Zhang, J.D. Qiu, *Electrochim. Acta* 56 (2011) 4231
13. J.D. Qiu, H.P. Peng, R.P. Liang, X.H. Xia, *Biosens. Bioelectron.* 25 (2010) 1447
14. F. Beckert , C. Friedrich , R. Thomann, R. Mülhaupt, *Macromolecules* 45 (2012) 7083
15. Y.K. Yang, C.E. He, R.G. Peng, A. Baji, X.S. Du, Y.L. Huang, X.L. Xie, Y.W. Mai, *J. Mater. Chem.* 22 (2012) 5666
16. S. P. Lonkar, A. Bobenrieth, J. D. Winter, P. Gerbaux, J.M. Raquez, P, Dubois, *J. Mater. Chem.* 22 (2012) 18124
17. K.H. Liao, Y.Q. Qian, C. W. Macosko, *Polymer* 53 (2012) 3756
18. M. Li, X.Y. Huang, C. Wu, H.P. Xu, P.K. Jiang, T. Tanaka, *J. Mater. Chem.* 22 (2012) 23477
19. L.P. Yang, J.H. Kong, W.A. Yee, W.S. Liu, S.L. Phua, C.L. Toh, S. Huang, X.H. Lu, *Nanoscale* 4 (2012) 4968
20. T. Kuila, S. Bose, C.E. Hong, M.E. Uddin, P. Khanra, N.H. Kim, et al. *Carbon* 2011 (49) 1033
21. S. Bose, T. Kuila, M.E. Uddin, N.H. Kim, A.K.T. Lau, J.H. Lee, *Polymer* 2010 (51) 5921
22. A. Gutés, B. Hsia, A. Sussma, W. Mickelson, A. Zettl, C. Carraro, R. Maboudian, *Nanoscale* 4 (2012) 438
23. D.X. Ye, L.Q. Luo, Y.P. Ding, B.D. Liu, X. Liu, *Analyst* 137 (2012) 2840
24. Y. Fan, X. Yang, C.P. Yang, J.H. Liu, *Electroanalysis* 24 (2012) 1334
25. C.H. Wu, C.H. Wang, M.T. Lee, J.K. Chang, *J. Mater. Chem.* 22 (2012) 21466
26. A. Galal, N. F. Atta, E. H. El-Ads, *Talanta* 93 (2012) 264
27. C.L. Li, Y. Su, X.Y. Lv, H.L. Xia, H.J. Shi, X.G. Yang, J.Q. Zhang, Y.J. Wang, *Biosens. Bioelectron.* 38(2012) 402
28. W.J. Lian, S. Liu, J.H. Yu, X.R. Xing, J. Li, M. Cui, J.D. Huang, *Biosens. Bioelectron.* 38 (2012) 163
29. N. German, A. Ramanavicius, J. Voronovic, A. Ramanaviciene, *Colloids and Surfaces A* 413 (2012) 224
30. K. K. Reddy, K. V. Gobi, *Electrochim. Acta* 78 (2012) 109
31. C.S. Shan, H.F. Yang, D.G. Han, Q.X. Zhang, A. Ivaska, L. Niu, *Biosens. Bioelectron.* 25 (2010) 1070
32. K.J. Huang, D.J. Niu, X. Liu, Z.W. Wu, Y. Fan, Y.F. Chang, Y.Y. Wu, *Electrochim. Acta* 56 (2011) 2947
33. W.S. Hummers, R.E. Offeman, *J. Am. Chem. Soc.* 80 (1958) 1339
34. E. Laviron, *J. Electroanal. Chem.* 101 (1979) 19
35. R.W. Murray, in: A.J. Bard (Ed.), *Electroanalytical Chemistry*, vol. 13, Marcel Dekker, New York(1984)
36. A.M. Bond, *Modern Polarographic Methods in Analytical Chemistry*, Marcel Dekker, New York(1980)

37. A. Safavi, F. Farjami, *Anal. Biochem.* 402 (2010) 20
38. Q. Lu, X.C. Dong, L.J. Li, X. Hu, *Talanta* 82 (2010) 1344
39. Y.Y. Zhang, R. Yuan, Y.Q. Chai, Y. Xiang, C.L. Hong, X.Q. Ran, *Biochem. Eng. J.* 51 (2010) 102
40. F. Guo, X.X. Xu, Z.Z. Sun, J.X. Zhang, Z.X. Meng,W. Zheng, H.M. Zhou, B.L.Wang, Y.F. Zheng, *Colloids and Surfaces B* 86 (2011) 140
41. F. Gao, Z. Yao, Q.A. Huang, X.X. Chen, X.Y. Guo, Q.Q. Ye, L. Wang, *Colloids and Surfaces B* 82 (2011) 359
42. J.D. Qiu, S.G. Cui, R.P. Liang, *Microchim. Acta* 171 (2010) 333